

Towards the Web of Quantum Chaos Diagnostics

Arpan Bhattacharyya,^{1,*} Wissam Chemissany,^{2,†} S. Shajidul Haque,^{3,‡} and Bin Yan^{4,5,§}

¹*Center for Gravitational Physics, Yukawa Institute for Theoretical Physics (YITP), Kyoto University, Kitashirakawa Oiwakecho, Sakyo-ku, Kyoto 606-8502, Japan.*

²*Institute for Quantum Information and Matter, California Institute of Technology, 1200 E California Blvd, Pasadena, CA 91125, USA.*

³*Department of Mathematics and Applied Mathematics,*

University of Cape Town, Private Bag, Rondebosch, 7701, South Africa.

⁴*Center for Nonlinear Studies, Los Alamos National Laboratory, Los Alamos, NM 87544, USA*

⁵*Theoretical Division, Los Alamos National Laboratory, Los Alamos, NM 87544, USA*

We study the connections between three quantities that can be used as diagnostics for quantum chaos, i.e., the out-of-time-order correlator (OTOC), Loschmidt echo (LE), and complexity. We generalize the connection between OTOC and LE for infinite dimensions and extend it for higher-order OTOCs and multi-fold LEs. Novel applications of this intrinsic relation are proposed. We also propose a relationship between a specific circuit complexity and LE by using the inverted oscillator model. These relationships signal a deeper connection between these three probes of quantum chaos.

CONTENTS

I. Introduction	1
II. Loschmidt Echo and OTOC	2
A. 4-point OTOC and Loschmidt Echo	2
1. Loschmidt Echo	2
2. 4-point OTOC	2
3. Bridging out the 4-point OTOC and the Loschmidt Echo	3
B. 2k-OTOC and 2(k-1)-fold Echo	3
C. Infinite dimensional generalization	5
D. Application I: Robust Witness of Scrambling	5
E. Application II: Shockwave and Loschmidt Echo	5
1. Echo evolution, Precursors and black holes	6
2. Single Shock	6
3. Multiple Shocks	7
4. The triangle links	7
5. Perspectives from infinite dimensional continuous variable systems	8
III. Loschmidt Echo and Complexity	10
A. Introducing Complexity	10
B. LE-Complexity connection	10
IV. Discussion	11
Acknowledgments	12
Author Contributions	12
A. Mathematical Gear Oils	12
References	13

I. INTRODUCTION

The quest of a quantum version for a classical chaos has gained too much momentum over the last few years. Interested readers are referred to [1] and the references therein. The reason is that the sought-after formulation of quantum chaos has appeared to be versatile entering many branches in theoretical and experimental physics. De facto, quantum chaos has found applications and received considerable attention across physical disciplines such as condensed matter physics, quantum information theory and high energy physics, in particular, in the context of black hole and holography [2]. Several diagnostic tools have been proposed to quantify these diverse aspects.

Over the time, the endeavors to improve the current diagnostic gadgets and develop new ones have gone a long way. The out-of-time-order correlator OTOC [3, 4] has been intensively utilized to examine chaotic phenomena leading to a significant and profound understanding for long-standing problems. Loschmidt Echo (LE), introduced as another powerful toolkit [5, 6], has also played a pivotal role in demystifying the deep structure of (quantum) chaos. Very recently, the notion of quantum/computational complexity has joined the club of quantum chaos diagnostics [7–10]. In [11], the authors shown that a particular type of complexity, namely circuit complexity[12, 13], can capture equivalent information as the OTOC.

There are serious indications that the proposed chaos *quantifiers* are related. For instance, there had been a strong belief that OTOC and LE are somehow connected due to the intrinsic echo nature of the OTOC. Indeed, in [14] a major step has been taken to establish such a link at all time scales. It is worth mentioning that, previously there had been several attempts [15, 16] to achieve the same goal, but all of them are resorted to some variants of the OTOC or specific choice of operators.

Our actual work can be regarded as the starter of the program that targets toward a complete web of quantum chaos diagnostics. The aim of this paper is two-fold;

* bhattacharyya.arpan@yahoo.com

† wissamch@caltech.edu

‡ shajidhaque@gmail.com

§ byan@lanl.gov

i) first, generalize the OTOC-LE connection of [14] for infinite dimensional system and extend it to k multi-fold and provide examples, ii) second, understand the triangle of relations between, OTOCs, LE and complexity.

It is worth emphasizing that we have only examined the LE-complexity relation in the context of single inverted oscillator and a specific LE. In the discussion section we shall comment and speculate on the possible ways to go beyond this example and highlight future directions.

II. LOSCHMIDT ECHO AND OTOC

We first start with an introduction to the Loschmidt echo and the regular 4-point OTOC. We will then discuss the general properties of these two quantities, as well as the intrinsic connection between them. Our first result is to generalize the link between the regular OTOC and LE to higher-order OTOCs and a echo quantity with multiple loops. This leads to a range of novel applications.

A. 4-point OTOC and Loschmidt Echo

1. Loschmidt Echo

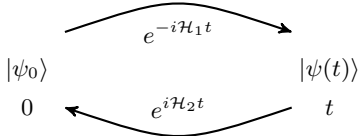


FIG. 1. LE as an echo quantity measures how much a quantum state is recovered by an imperfect time reversal.

The LE is formally defined as [6]

$$M(t) = \langle \psi_0 | e^{i\mathcal{H}_2 t} e^{-i\mathcal{H}_1 t} | \psi_0 \rangle,$$

where $|\psi_0\rangle$ is the initial state of a quantum system, \mathcal{H}_1 and \mathcal{H}_2 are two slightly different Hamiltonian, e.g., $\mathcal{H}_1 = \mathcal{H}_0$ is the unperturbed Hamiltonian, and $\mathcal{H}_2 = \mathcal{H}_0 + V$ with V a small perturbation. In the literature, the LE could also refer to the square of the magnitude of the above quantity to remove the phase which is typically not essential.

There are two ways to interpret the LE. The first is to think of it as an “echo” process; it qualifies how much of the complex system is recovered upon applying an imperfect time-reversal, as sketched in Fig. II A 1.

The other way is to interpret it as the overlap (the “distance”) between two wavefunctions (“trajectories”) evolving under slightly different dynamics. This in analogy to the classical notion of chaos, though in the latter case perturbations are applied to the initial condition in the classical phase space, while in the quantum case the perturbations are applied to the Hamiltonian. (Due to the fundamental unitary dynamics in quantum systems, any

small perturbations on the initial wavefunctions remain unchanged during time evolution.) In this sense, the LE is related to the *butterfly effect*, so one can consider it as a type of diagnostic tools for chaos.

2. 4-point OTOC

The regular 4-point OTOC is formally defined as

$$F_\beta(t) = \langle W^\dagger(t) V^\dagger(0) W(t) V(0) \rangle_\beta,$$

Here the average is taken over a thermal state at inverse temperature β . W and V are two local operators on distinct local subsystems. $W(t) \equiv e^{-iHt} W e^{iHt}$ is the Heisenberg evolution of operator W . The OTOC has been extensively studied in various context and different variants of it has been proposed. For instance, taking average over pure states, or choosing global operators [17, 18].

We note the following universal features of the OTOC:

- When W and V are both Hermitian and unitary, the OTOC is related to the squared commutator

$$F_\beta(t) = 1 - \frac{1}{2} \langle [W(t), V]^2 \rangle.$$

Two local operator W and V commute at $t = 0$. The Heisenberg evolution converts $W(t)$ into a global operator; the commutator hence fails to vanish and induces decay of the OTOC. For chaotic dynamics the OTOCs exhibits fast decays.

- The OTOC has several decay regimes. At early stage before the Ehrenfest time scale (scrambling regime), the decay of OTOC is manifested as an exponential growth, $1 - \delta e^{\lambda t}$, where $\delta \ll 1$. This type of decay certainly does not converge, and will switch to a pure exponential decay before saturation. In the asymptotic regime the OTOC typically shows model-dependent power law behaviors. In the scrambling regime, the exponential growth rate is conjectured to be bounded by the temperature, i.e., $\lambda \leq 2\pi/\beta$ from holography [19].
- Different choices of operators of W and V share common features of their OTOCs. For complex enough systems, the OTOC is not sensitive to the particular form of the operators, as long as they are generic, e.g., random operators. This makes it possible to extract the universal properties of the OTOC by averaging over all operators of given subsystems. In the following sections we explore the consequences of this averaging procedure.

3. Bridging out the 4-point OTOC and the Loschmidt Echo

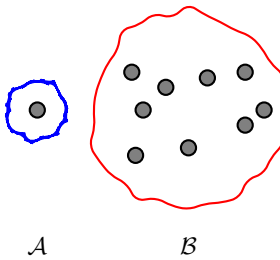


FIG. 2. Local structure of the total system and the choice of subsystems in the OTOC.

As noted in the previous section, the insensitivity to the choice of operators allows one to extract the universal features of OTOC by taking the average over a given set of operators. The average procedure has been considered for different variants of the OTOCs. When restricted to the original form with local operators, there exists a strong relation between the Loschmidt echo and the 4-point OTOC which is the resemblance of the latter to the thermal average of the Loschmidt echo signal.

Without losing the local structure of a many-body system, the supports of two operators W and V are chosen as two distinct subsystems \mathcal{A} and \mathcal{B} , where \mathcal{A} is a small subsystem, while \mathcal{B} is the complement of \mathcal{A} to the total system, as illustrated in Fig. 2. We then take the average of the two operators over the set of all unitaries on the two fixed subsystems with the “largest randomness”, i.e., with respect to the Haar measure.

It has been demonstrated in Ref. ([14]) that the OTOC and LE are ultimately related as

$$\begin{aligned} \int_{Haar} dW dV \langle W^\dagger(t) V^\dagger W(t) V \rangle_{\beta=0} \\ \approx \left| \langle e^{i\mathcal{H}_B} \times e^{-i(\mathcal{H}_B+V)t} \rangle_{\beta=0} \right|^2. \end{aligned}$$

Here the Hamiltonian of the larger subsystem \mathcal{B} plays the role as the unperturbed Hamiltonian; and the perturbation V naturally emerges from the interaction between the two subsystems. For proper regularization of the thermal state, this relation generalizes to finite temperature as well [14].

In the following section, we will attempt to generalize this work and bridge 2k-point OTOC to the k-fold Loschmidt echo.

B. 2k-OTOC and 2(k-1)-fold Echo

In this section, we will generalize the link between the 4-point OTOC and LE to higher order OTOCs and multi-fold LE. We first give a formal definition of the 2k-point

OTOC. We then demonstrate that it is linked to a LE with $2(k-1)$ forward and backward loops.

The regular 4-point OTOC,

$$\langle W^\dagger(t) V^\dagger(0) W(t) V(0) \rangle,$$

probes the spreading of the local operator W over the entire system. The work of Refs. [20, 21] suggests the study of the generalized 2k-OTOC, defined as

$$\begin{aligned} \langle \mathcal{W}^\dagger V^\dagger(0) \mathcal{W} V(0) \rangle = \langle W_1^\dagger(t_1) \dots W_{k-1}^\dagger(t_{k-1}) \\ V^\dagger(0) W_{k-1}(t_{k-1}) \dots W_1(t_1) V(0) \rangle, \end{aligned} \quad (1)$$

where $\mathcal{W} \equiv W_{k-1}(t_{k-1}) \dots W_1(t_1)$ indicates the ordering of the operators in the correlator.

There are other types of generalized definitions of the 2k-OTOC, such as the ones used to probe k-designs in Ref. [20], or the one connected to the spectral form factors in Ref. [22]. The operators in the correlator could be interpreted as either global (e.g., as in Refs. [20, 22]) or local operators (e.g., as in Ref. [21]) for different purposes.

At the moment, we first focus on the most restricted sense, i.e., the operator W_k 's are all local operators applying on distinct local (and small) subsystems, such that the 2k-OTOC (1) probes the scrambling of multiple local perturbations. We choose V as an operator on the complement of the $k-1$ local subsystems.

We denote

$$W_k(t_k) \equiv U_k^\dagger W_k U_k \equiv \tilde{W}_k,$$

where $U_k = e^{iHt_k}$ represents (local) Hamiltonian evolution.

Consider the averaged 2k-OTOC with respect to the Haar integral at infinite temperature,

$$\begin{aligned} \int_{Haar} dW_1 \dots dW_{k-1} dV \langle \tilde{W}_1^\dagger \dots \tilde{W}_{k-1}^\dagger V^\dagger \\ \tilde{W}_{k-1} \dots \tilde{W}_1 V \rangle_{\beta=0} \\ = \frac{1}{d} Tr \int_{Haar} dW_1 \dots dW_{k-1} dV (\tilde{W}_1^\dagger \dots \tilde{W}_{k-1}^\dagger V^\dagger \\ \tilde{W}_{k-1} \dots \tilde{W}_1 V) \end{aligned}$$

The particular ordering of operators in the integrand allows us to perform the integral one-by-one, e.g., the innermost integral for the W_{k-1} operators can be computed first (See Appendix A for Haar average over subsystems.):

$$\begin{aligned} & \int dW_{k-1} \left(\tilde{W}_1^\dagger \dots \tilde{W}_{k-1}^\dagger V^\dagger \tilde{W}_{k-1} \dots \tilde{W}_1 V \right), \\ &= \int dW_{k-1} \left(\tilde{W}_1^\dagger \dots \tilde{W}_{k-2}^\dagger U_{k-1}^\dagger W_{k-1}^\dagger \right. \\ & \quad \left. U_{k-1} V^\dagger U_{k-1}^\dagger W_{k-1} U_{k-1} \tilde{W}_{k-2} \dots \tilde{W}_1 V \right), \\ &= \frac{1}{d_{k-1}} \tilde{W}_1^\dagger \dots \tilde{W}_{k-2}^\dagger U_{k-1}^\dagger Tr_{k-1} \left(U_{k-1} V^\dagger U_{k-1}^\dagger \right) \\ & \quad U_{k-1} \tilde{W}_{k-2} \dots \tilde{W}_1 V, \end{aligned}$$

where Tr_{k-1} represents the partial trace over the subsystem $k-1$.

Performing the integral for all the W operators gives

$$\begin{aligned} & \frac{1}{d} Tr \int_{Haar} dW_1 \dots dW_{k-1} dV \left(\tilde{W}_1^\dagger \dots \tilde{W}_{k-1}^\dagger V^\dagger \right. \\ & \quad \left. \tilde{W}_{k-1} \dots \tilde{W}_1 V \right) \\ &= \frac{1}{d} \frac{1}{d_1 \dots d_{k-1}} Tr \int dV \quad U_1^\dagger Tr_1 \left(U_1 \dots U_{k-2}^\dagger \right. \\ & \quad \left. Tr_{k-2} \left(U_{k-2} U_{k-1}^\dagger Tr_{k-1} \left(U_{k-1} V^\dagger U_{k-1}^\dagger \right) U_{k-1} U_{k-2}^\dagger \right. \right. \\ & \quad \left. \left. U_{k-2} \dots U_1^\dagger \right) U_1 V \right) \\ &= \frac{1}{d} \frac{1}{d_1 \dots d_{k-1}} Tr \int dV \underbrace{Tr_1 \left\{ U_1 \dots U_{k-2}^\dagger Tr_{k-2} \left[U_{k-2} U_{k-1}^\dagger \right. \right.}_{A} \\ & \quad \left. \left. Tr_{k-1} \left(U_{k-1} V^\dagger U_{k-1}^\dagger \right) U_{k-1} U_{k-2}^\dagger \right] U_{k-2} \dots U_1^\dagger \right\} \underbrace{U_1 V U_1^\dagger}_{B} \dots \end{aligned}$$

Using the same trick provided in the 4-point OTOC, [14], the partial traces in piece- A can be evaluated one-by-one (see Appendix A). For instance, the inner-most partial trace is

$$\begin{aligned} Tr_{k-1} \left(U_{k-1} V^\dagger U_{k-1}^\dagger \right) &= Tr_{k-1} \left(e^{-iHt_{k-1}} V^\dagger e^{iHt_{k-1}} \right) \\ &\approx d_{k-1} \times \frac{1}{N_{k-1}} \sum_{P_{k-1}} e^{-i(H_V + P_{k-1})t_{k-1}} V^\dagger e^{i(H_V + P_{k-1})t_{k-1}}. \end{aligned}$$

Denote N_{k-1} the number of different P_{k-1} operators, which serve as the perturbations. The summation range over all of them. These noisy operators emerge from the interaction between the $k-1$'s subsystem with the rest of the total system (See Appendix A for details).

Note 1: The LHS of the above equation, after tracing over the $(k-1)$ 'th subsystem, is an operator that involves not only the subsystem- V , but also subsystems $1, 2, \dots, k-2$. However, we assume that it only evolves (under noises) in subsystem- V and it does not “leak” to other subsystems.

Note 2:

$$U_{k-2} U_{k-1}^\dagger \equiv e^{-iHt_{k-2}} e^{iHt_{k-1}} = e^{-iH(t_{k-2} - t_{k-1})},$$

the above procedure for partial tracing can be repeated to all partial traces, which give the expression for A :

$$\begin{aligned} A &= d_1 \dots d_{k-1} \frac{1}{N_1 \dots N_{k-1}} \sum_{P_1, \dots, P_{k-1}} \underbrace{e^{-i(H_V + P_1)(t_1 - t_2)} \dots}_{D} \\ & \quad \underbrace{e^{-i(H_V + P_{k-2})(t_{k-2} - t_{k-1})} e^{-i(H_V + P_{k-1})(t_{k-1} - t_0)}}_{D} V^\dagger D^\dagger. \end{aligned}$$

Finally,

$$\begin{aligned} & \frac{1}{d} \frac{1}{d_1 \dots d_{k-1}} Tr \int dV AB \\ &= \frac{1}{d} \frac{1}{N_1 \dots N_{k-1}} Tr \int dV \sum_{P_1, \dots, P_{k-1}} DV^\dagger D^\dagger U_1 V U_1^\dagger \end{aligned}$$

As has been discussed before, $U_1 V U_1^\dagger$ is a global operator, while $DV^\dagger D^\dagger$ is an operator with support on system- V only. Thus the trace in the above equation can be evaluated with two partial traces $Tr = Tr_V Tr_{\bar{V}}$, namely, $Tr[(M_V \otimes \mathbb{I}_{\bar{V}})N_{V\bar{V}}] = Tr_V [M_V Tr_{\bar{V}}(N_{V\bar{V}})]$. Denote $d_1 \dots d_{k-1} \equiv d_{\bar{V}}$, which is the dimension of the Hilbert space of the subsystem complementary to subsystem- V . The above equation continues as

$$\begin{aligned} &= \frac{1}{d} \frac{1}{N_1 \dots N_{k-1}} \sum_{P_1, \dots, P_{k-1}} Tr_V \left[\int dV DV^\dagger D^\dagger Tr_{\bar{V}} \left(U_1 V U_1^\dagger \right) \right], \\ &= \frac{1}{N_1 \dots N_{k-1}} \frac{1}{d_V} \frac{1}{d_{\bar{V}}} \sum_{P_1, \dots, P_{k-1}} Tr_V \left[\int dV DV^\dagger D^\dagger \right. \\ & \quad \left. \left(\frac{1}{N_0} \sum_{P_0} e^{-i(H_V + P_0)t_1} V e^{i(H_V + P_0)t_1} \right) \right] \\ &= \frac{1}{N_0 \dots N_{k-1}} \frac{1}{d_V} \sum_{P_0, \dots, P_{k-1}} Tr_V \left(\int dV DV^\dagger D^\dagger e^{-i(H_V + P_0)t_1} \right. \\ & \quad \left. V e^{i(H_V + P_0)t_1} \right), \\ &= \frac{1}{N_0 \dots N_{k-1}} \frac{1}{d_{\bar{V}}^2} \sum_{P_0, \dots, P_{k-1}} \left| Tr \left(e^{i(H_V + P_0)t_1} D \right) \right|^2 \\ &= \frac{1}{N_0 \dots N_{k-1}} \frac{1}{d_{\bar{V}}^2} \sum_{P_0, \dots, P_{k-1}} \left| Tr \left[e^{i(H_V + P_0)t_1} \right. \right. \\ & \quad \left. \left. e^{-i(H_V + P_1)(t_1 - t_2)} \dots e^{-i(H_V + P_{k-2})(t_{k-2} - t_{k-1})} \right. \right. \\ & \quad \left. \left. e^{-i(H_V + P_{k-1})(t_{k-1} - t_0)} \right] \right|^2. \end{aligned}$$

P_1, \dots, P_{k-1} are perturbations emerge from the tracing our the subsystems $-1, \dots, k-1$; and they have, respectively. P_0 emerges from tracing out the subsystem \bar{V} . For complex systems, the structure of these perturbation operators are not essential. Hence, we can eliminate the average over all the perturbations and treat each P_i as a constant perturbation instead of a variable. The above

equation finally turns out to be

$$\begin{aligned}
&= \frac{1}{d_V^2} \left| \text{Tr} \left[e^{i(H_V+P_0)t_1} e^{-i(H_V+P_1)t_1} e^{i(H_V+P_1)t_2} \right. \right. \\
&\quad \left. \left. \dots e^{-i(H_V+P_{k-2})t_{k-2}} e^{i(H_V+P_{k-2})t_{k-1}} e^{-i(H_V+P_{k-1})t_{k-1}} \right] \right|^2, \\
&= \left| \left\langle \left[e^{i(H_V+P_0)t_1} e^{-i(H_V+P_1)t_1} e^{i(H_V+P_1)t_2} \right. \right. \right. \\
&\quad \left. \left. \dots e^{-i(H_V+P_{k-2})t_{k-2}} e^{i(H_V+P_{k-2})t_{k-1}} \right. \right. \\
&\quad \left. \left. e^{-i(H_V+P_{k-1})t_{k-1}} \right] \right\rangle_{\beta=0} \right|^2.
\end{aligned}$$

This is the expected Loschmidt echo with $2(k-1)$ loops.

C. Infinite dimensional generalization

The previous discussions focus on finite dimensional Hilbert spaces¹. In this section we argue that the OTOC-LE connection can be generalized to infinite dimension. The key ingredient is the Haar integral for unitary operators U on an infinite dimensional Hilbert space, $\int d\mu(U) U^\dagger O U$, where O is a trace-class operator and μ is the Haar measure.

Here we consider the right Haar measure, which, by definition, is invariant under transformation $U \rightarrow UV$, i.e., $\mu(UV) = \mu(U)$ for any unitary operator V , which implies

$$\int d\mu(U) U^\dagger O U = V^\dagger \left(\int d\mu(U) U^\dagger O U \right) V.$$

This means that the Haar-averaged operator is proportional to the identity operator I .

In finite dimensions, its trace can be computed as

$$\text{Tr} \int d\mu(U) U^\dagger O U = \int d\mu(U) \text{Tr}(O).$$

Haar measure is unique up-to a constant multiplication factor; and the unitary groups on finite dimensional Hilbert spaces have finite measures. This allows us to normalize the Haar measure by choosing $\int d\mu = 1$. Under this convention, the averaged operator has the representation

$$\int d\mu(U) U^\dagger O U = \frac{1}{d} \text{Tr}(O) I,$$

where d is the dimension of the Hilbert space.

For infinite dimensions, the Haar measure is not normalizable, and hence the averaged operator is not trace-class anymore. However, we are interested in the case where the averaged operator is still bounded (the OTOC takes finite values). In this case, the Haar averaged operator can be fixed as a constant multiplied by the identity, $c(O)I$. The functional c must be linear and invariant under unitary transformation, i.e., $c(O) = c(U^\dagger O U)$. By Riesz representation theorem, it is determined, up-to a multiplication factor, to be the trace, i.e., $c(O) \propto \text{Tr}(O)$. We have the freedom to remove the pre-factor by absorbing it into the definition of the Haar measure. Under this convention, the desired integral for the Haar average matches precisely with the one in finite dimensions. Once this infinite dimensional Haar integral is evaluated, the OTOC-LE connection follows in the same manner as in the finite dimensional case.

If we average the OTOC over a given group of unitaries $\{U_g\}$, rather than performing the average over all unitary operators with respect to Haar measure, we can firmly say that the OTOC-LE connection holds as well, as long as the group average, up-to a constant multiplication factor which can be removed by re-scaling the measure, gives the same result as the Haar average, namely,

$$\int dU_g U_g^\dagger O U_g \propto \int d\mu_{\text{Haar}}(U) U^\dagger O U = \text{Tr}(O) I.$$

In other words, the group $\{U_g\}$ is an analog of the unitary 1-design in finite dimensions.

As an example, consider the Heisenberg group $\{U(q_1, q_2) = e^{i(q_1 \hat{x} + q_2 \hat{p})}\}$, where \hat{x} and \hat{p} are the canonical position and momentum operator, q_1 and q_2 are real numbers.

To show that the Heisenberg group is a unitary 1-design, we will need to prove, for any trace-class operator O ,

$$D \equiv \int \frac{dq_1}{2\pi} \int dq_2 U^\dagger(q_1, q_2) O U(q_1, q_2) = \text{Tr}(O) I.$$

This is equivalent to showing that the above operator D in the position representation has elements

$$\begin{aligned}
\langle x | D | x' \rangle &= \int \frac{dq_1}{2\pi} \int dq_2 \langle x | U^\dagger(q_1, q_2) O U(q_1, q_2) | x' \rangle \\
&= \int dx_1 \int dx_2 \int \frac{dq_1}{2\pi} \int dq_2 \\
&\quad \langle x | U^\dagger(q_1, q_2) | x_1 \rangle \langle x_1 | O | x_2 \rangle \langle x_2 | U(q_1, q_2) | x' \rangle \\
&= \int dx_1 \int dx_2 \delta(x - x') \delta(x_1 - x_2) \langle x_1 | O | x_2 \rangle \\
&= \text{Tr}(O) \delta(x - x').
\end{aligned}$$

D. Application I: Robust Witness of Scrambling

The OTOC is designed as a diagnostic for chaos. For chaotic systems the OTOC decays rapidly and converges to a persistent small value. In contrast, for regular systems the OTOC typically exhibits oscillatory behaviors,

¹ For 2pt OTOC, a possible generalization for infinite dimensional Hilbert spaces has been studied in [23].

with a finite recurrent time. OTOC has been experimentally detected in various platforms [24–26]. However, realistic experiments suffers from decoherence caused by errors and couplings to the environments. As a consequence, integrable systems also display rapid decaying OTOC, and hence hinders us from distinguishing regular and chaotic dynamics. Several protocols have been proposed to robustly detect of the OTOC decay in realistic, decoherent experiments. For example, interested readers are referred to [27] and the citations and references of it. Here, as the first novel application of the higher-order OTOC-LE connection, we propose to use the $2k$ -point OTOC to probe the chaotic signature of a system.

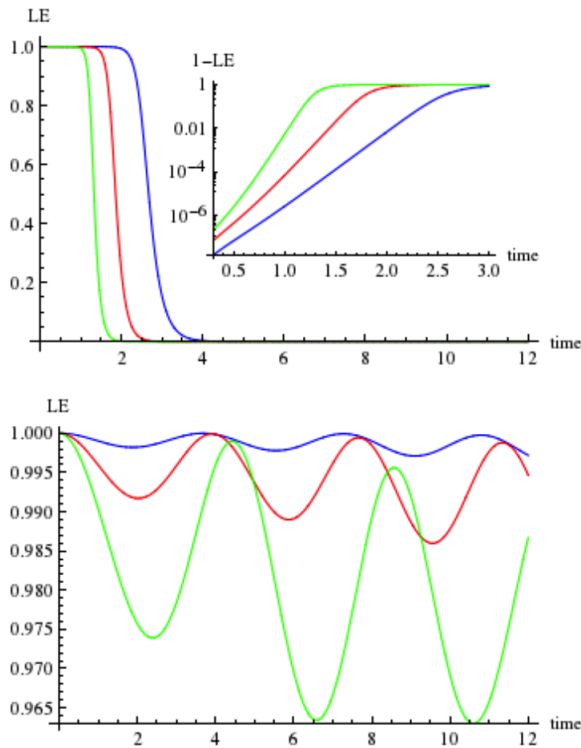


FIG. 3. Time evolution of the multi-fold LE for inverted (upper) and regular (lower) oscillator ($m = 1, \lambda = 0.1$ (regular), 5 (inverted), $\delta\lambda = 0.1$ (regular), 0.001 (inverted)). Inset shows the early exponential growth of the LE of the inverted oscillator. Blue, red and green curves correspond to the LE with $2, 4$, and 6 loops.

The argument is straightforward. Due to the connection to multi-fold LE, the decay rate of the $2k$ -point OTOC is roughly proportional to the number of loops in the LE. For chaotic systems the observed decay of the OTOC is much sharpened when we add more loops into the evolution. However, for regular systems, after each pair of forward and backward loop, the LE goes back to the initial state at the recurrent time. Adding more loops would not change the recurrence of the LE. Thus, even with the presence of decoherence, the time scale of regular systems will not be altered by adding multiple loops.

To demonstrate this fact, we study the multi-fold LE evolution of a simple model problem, namely, a single harmonic oscillator

$$H = \frac{1}{2}p^2 + \frac{\Omega^2}{2}x^2, \text{ where } \Omega^2 = m^2 - \lambda.$$

The oscillator can be tuned to the regular and chaotic regime by changing the value of λ , i.e., for $\lambda < m^2$ the oscillator is simple, while for $\lambda > m^2$ the oscillator is inverted and chaotic. In each loop of the LE, we add a small perturbation to the frequency, $\Omega' = \Omega + \delta$. The initial state of the oscillator is prepared as a Gaussian state, $\psi(x, t = 0) = \mathcal{N} \exp(-\frac{\omega_r x^2}{2})$, where $\omega_r = m$, and \mathcal{N} is the normalization factor. Following the procedure in [11], the LE can be computed exactly. In Fig. 1 we show the evolution of the LE for both regular and chaotic regime. For the inverted oscillator, the LE exhibits clear early-time exponential growth. The growth rate is roughly proportional to the number of loops. For the oscillator in the integrable regime, the recurrent time does not show dramatic changes when adding more loops to the LE.

E. Application II: Shockwave and Loschmidt Echo

We further illustrate the relation OTOC-LE with a brief application from AdS/CFT correspondence. We shall examine this for an AdS eternal black hole Fig.4. This subsection is primarily based on the following work [28–35] and references therein. We shall also shed some light into the possible link that may exist between OTOCs, LE and quantum complexity which we will elaborate on in the next section.

1. Echo evolution, Precursors and black holes

Let's consider two entangled black holes connected by an Einstein-Rosen bridge, aka wormhole Fig.5. The holographic description of the wormhole volume is quantified by the complexity of the quantum state of the dual pair of CFTs at time t . For a given thermofield double state, we can evolve, for instance, the left side back in time for a time $\Delta t_L = -t_w$ and then apply a simple localized precursor perturbation W_L that adds a thermal quantum; a localized packet of energy in the left side. Then, we evolve this state forward in time, $\Delta t_L = t_w$ (see Fig.6). Due to the fact that the quantum state loses its memory, the left target state has to differ from the left initial state.

In AdS spacetime, this energy source starts to warp the spacetime near the horizon by creating a gravitational shockwave which expands away from the source, and remains highly energetic for most of its worldline. This kick changes the geometry and leads to a larger wormhole compared to the initial one. More precisely, the wormhole owes its growth to the gravitational back-reaction on the shape of the geometry (or alternatively to the hop and displacement of the trajectories crossing the shockwave

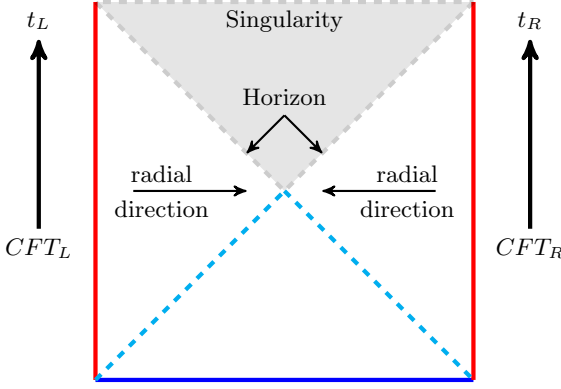


FIG. 4. Penrose diagram of an eternal AdS-Schwarzschild black hole.

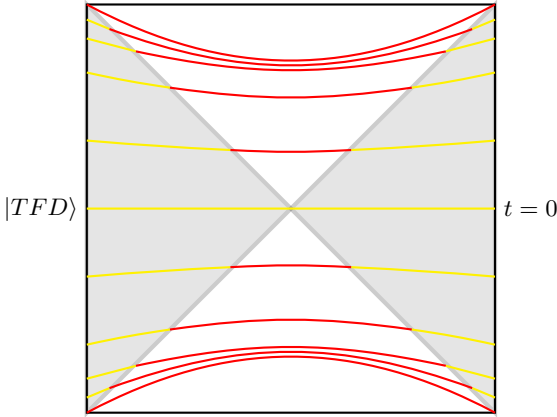


FIG. 5. The dark red surfaces are the maximal spacelike slices foliating the diagram behind the horizon and representing the wormhole.

Fig.7). This corresponds, on the CFT side, to a greater decay for the correlation between the two different sides of the thermofield-double state. Consequently, one infers that there exists a correspondence between the amount of energy the shockwaves produce and the rate of decay of the correlations. In what follows, we shall provide a rough picture as to how this might play out.

2. Single Shock

Let us apply the *echo* evolution $e^{-iH_L t_w} W_L e^{iH_L t_w}$ to the thermofield-double state:

$$|w\rangle = e^{-iH_L t_w} W_L e^{iH_L t_w} |TFD\rangle \quad (2)$$

$$= W_L(t_\omega) |TFD\rangle \quad (3)$$

where for any single sided operator (precursor) W , $W_L = W \otimes \mathbb{I}$ and $W_R = \mathbb{I} \otimes W$. The operator $W_L(t_\omega)$ is a Schrödinger picture operator acting at time $t = 0$. The effect of $W_L(t_\omega)$ amounts to adding at t_ω a thermal quantum to the left side. Note that despite the fact that the thermal quantum, being localized low energy perturba-

tion, created by $W_L(t_\omega)$, feeds a tiny bit of energy to the black hole, for most of its worldline it is astronomically energetic shockwave.

The two-sided correlator is found to be (see for instance [35])

$$\begin{aligned} & \langle w | V_L \otimes V_R^T | w \rangle \\ &= \langle TFD | e^{-iH_L t_w} W_L^\dagger e^{iH_L t_w} V_L \otimes V_R^T e^{-iH_L t_w} W_L e^{iH_L t_w} | TFD \rangle, \\ &= \langle TFD | W_L^\dagger(-t_w) V_L \otimes V_R^T W_L(-t_w) | TFD \rangle, \\ &= \langle TFD | (W_L^\dagger(-t_w) \otimes \mathbb{I}) (V_L \otimes V_R^T) (W_L(-t_w) \otimes \mathbb{I}) | TFD \rangle, \\ &= \langle TFD | W_L^\dagger(-t_w) V_L W_L(-t_w) \otimes V_R^T | TFD \rangle. \end{aligned}$$

The transpose "T" is in the energy basis. The state is subject to the so-called operator pushing property by which we mean

$$\hat{W}_R |max\rangle = \hat{W}_L^T |max\rangle \quad (4)$$

with $|max\rangle$ being a maximally entangled state. Using (4), one can push V^T from the right to the left. One therefore can convert the two-sided correlator to a one-sided correlator, i.e.,

$$\begin{aligned} \langle w | V_L \otimes V_R^T | w \rangle_{\beta=0} &= \underbrace{\langle W_L^\dagger(-t_w) V_L W_L(-t_w) V_L \rangle_{\beta=0}}_{\text{correlation between the 2 sides after perturbation}} \\ &= \underbrace{\langle W_L^\dagger(-t_w) V_L W_L(-t_w) V_L \rangle}_{\text{4-point OTOC at time } -t_w} \\ &= \frac{1}{2^N} \text{Tr}(W_L^\dagger(-t_w) V_L W_L(-t_w) V_L). \end{aligned} \quad (5)$$

The negative time is not profoundly significant. Evolving the system according to negative time is expected to have the same behaviour as evolving it with positive time. As a matter of fact, the behaviour of the OTOC can be generic for different local operators. In this case for any thermal state the aforementioned argument may be extracted from $\langle W^\dagger(-t_w) VV(-t_w) V \rangle_\beta = \langle W^\dagger V(t) VV(t) \rangle_\beta$. The generalization of the previous claim to general temperature, for which the obtained OTOCs are thermally regulated, is straightforward [35].

3. Multiple Shocks

The lesson one can draw out from the previous single shock case is that the more shockwaves (energy) you feed the black hole with, the greater the decay of the OTOCs becomes. To create two shockwaves one needs to consecutively repeat the process introduced above twice, that is,

$$\begin{aligned} |w_{1,2}\rangle &= e^{-iH_L t_2} W_2 e^{iH_L t_2} e^{-iH_L t_1} W_1 e^{iH_L t_1} |TFD\rangle, \\ &= W_2(-t_2) W_1(-t_1) |TFD\rangle \\ &= W_{\text{multi}}(t_2, t_1) |TFD\rangle. \end{aligned}$$

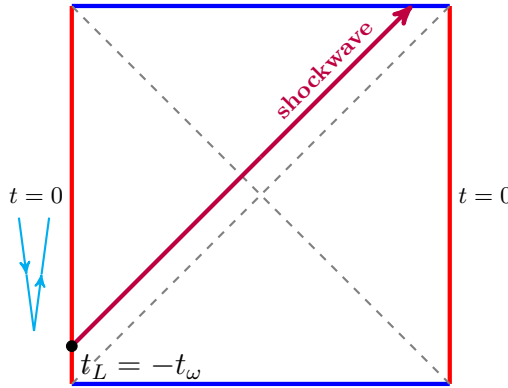


FIG. 6. The operator W_L creates an infalling quantum at $|t_w| >> t_*$, where t_* is the scrambling time. It undergoes a huge blue shift as it moves at the speed of light toward the horizon.

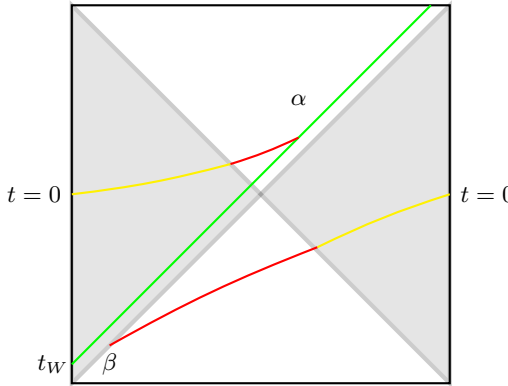


FIG. 7. In the absence of the shockwave the size of the maximal spacelike slice formed behind the horizon is null (it goes through the intersection point of the bifurcate horizon). Adding the shockwave allows the maximal slice to acquire a considerable volume as indicated by the red surfaces.

from which one can derive

$$\underbrace{\langle w_{1,2} | V_L \otimes V_R^T | w_{1,2} \rangle}_{\text{correlation between 2 sides after perturbing twice}} = \underbrace{\langle W_1^\dagger(-t_1) W_2^\dagger(-t_2) V_L W_2(-t_2) W_1(-t_1) V_L \rangle}_{\text{6-point OTOC}}.$$

Notice that we can get rid of the negative time because of the same previously mentioned reasons. This makes our claim true for the case of two shockwaves. Upon the application of multiple $(k-1)$ operators $W(t)$ on $|TFD\rangle$ (pictorially presented in Fig.8), One can write

$$|w_{1,2,\dots,k-1}\rangle = W_{\text{multi}}(t_{k-1}, \dots, t_1) |TFD\rangle, \quad (6)$$

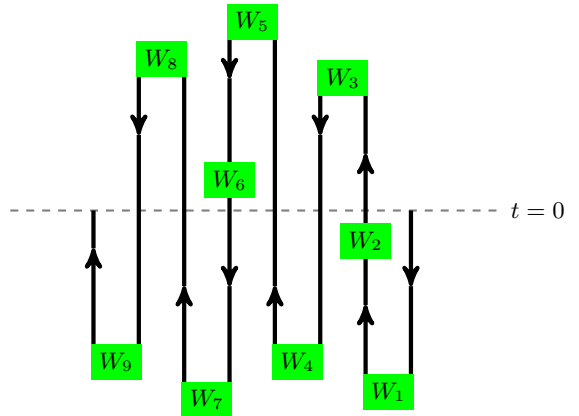


FIG. 8. Multifold echo with $2(k-1)$ loops. Each green insertion represents a tiny perturbation. The arrows point toward the order in which the precursors W_i 's apply.

from which one ought to obtain $2k$ -OTOC where $k > 1$, i.e.,

$$\underbrace{\langle w_{1,2,\dots,k-1} | V_L \otimes V_R^T | w_{1,2,\dots,k-1} \rangle}_{\text{correlation between 2 sides after perturbing (k-1) times}} = \underbrace{\langle W_1^\dagger(-t_1) \dots W_k^\dagger(-t_k) V_L W_k(-t_k) \dots W_1(-t_1) V_L \rangle}_{\text{2k-point OTOC}}.$$

4. The triangle links

As claimed above the shockwave has a large effect on the geometry. Without the shockwaves the volume of the maximal slice behind the horizon at $t = 0$ is null (it goes through the bifurcate horizon). Upon the creation of the shockwaves the spatial maximal slice, representing the wormhole connecting the two-sided entangled black holes, gains a significant volume. Roughly speaking, one can anticipate that the correlation exponentially decays with the size (length) $L(t)$ of the wormhole. Thus ²,

$$\langle w | V_L \otimes V_R^T | w \rangle_{\beta=0} \sim e^{-\frac{L(t)}{L_{\text{AdS}}}}. \quad (7)$$

Using (5), it yields

$$\langle W_L^\dagger(-t_w) V_L W_L(-t_w) V_L \rangle_{\beta=0} \sim e^{-\frac{L(t)}{L_{\text{AdS}}}}. \quad (8)$$

From the OTOC-LE connection, we have

$$\int_{\text{Haar}} dW dV \langle W_L^\dagger(t) V_L^\dagger W_L(t) V_L \rangle_{\beta=0} \approx |\langle e^{iH_L t} e^{-i(H_L + \Delta)t} \rangle|^2.$$

² We assume that the perturbations separately and successively act such that effect of W_i fills out the entire system before W_{i+1} kicks in.

This implies, roughly,

$$\left| \langle TFD | e^{iH_L t_w} W_L e^{-iH_L t_w} | TFD \rangle \right|^2 = \left| \langle TFD | w \rangle \right|^2.$$

We find that

$$\left| \langle TFD | w \rangle \right|^2 = \int_{\text{Haar}} dW dV e^{-l(t)/l_{AdS}}.$$

It has been conjectured by Susskind and companies that quantum complexity \mathcal{C} (precisely introduced in section III) is related to the size (length/volume) \mathcal{V} of the wormhole connecting the two entangled black holes, i.e., $\mathcal{C} = \frac{\mathcal{V}}{Gl_{AdS}}$. Combined all these together we end up with

$$e^{-iH_L t_w} W e^{iH_L t_w} |TFD\rangle = |w\rangle \quad (9)$$

$$\begin{aligned} &\Rightarrow \langle TFD | e^{iH_L t_w} e^{-i(H_L+V)t_w} | TFD \rangle = \langle TFD | w \rangle, \\ &\Rightarrow |\langle TFD | e^{iH_L t_w} e^{-i(H_L+V)t_w} | TFD \rangle|^2, \\ &= |\langle TFD | w \rangle|^2 \sim LE \sim e^{-L(t)/l_{AdS}} = e^{-\mathcal{C}}. \end{aligned} \quad (10)$$

This derivation involves only one single shockwave. However, one can incorporate multitude of shocks for which the one-fold LE is superseded by multi-fold LE and complexity associated with one localized precursor replaced by $\mathcal{C}[W_{multi}(t_{k-1}, \dots, t_1)]$ such that

$$2k\text{-OTOC} \sim e^{\frac{\tilde{L}(t)}{l_{AdS}}} \quad (11)$$

$$2k\text{-OTOC} = LE_{multi} \sim e^{-\mathcal{C}_{multi}}, \quad (12)$$

where $\tilde{L}(t)$ is the stretched length of the ERB (wormhole) behind the horizon.

5. Perspectives from infinite dimensional continuous variable systems

It has been established in [36] a relation between an operator's distribution in phase space and OTOCs in continuous variable (CV) system. Consider an operator that spreads in phase space having width/volume \mathcal{V} . The OTOC was found to be [36]

$$\mathcal{C}_2(\xi_1, \xi_2; t)_{\rho} \sim e^{-\mathcal{V}|\xi_2|^2}. \quad (13)$$

This OTOC-volume relation nourishes our belief in the previous claim that a large phase space volume, which can somehow be related to the real space wormhole volume/complexity, implies a greater decay of the OTOC. To derive (13) we shall introduce a few definitions and quantities. We begin by defining the displacement operator, the analog of the Pauli operator in discrete variables, for a simple harmonic oscillator (single mode CV system)

$$D(\xi_2, \xi_2) \equiv e^{[i(\xi_2 q - \xi_1 p)]}. \quad (14)$$

Such shifts operators, being e.g., elements of the Heisenberg group, form a complete basis and act on a coherent state in phase space. For N -mode CV system they read

$$D(\xi) = e^{i\mathbf{x}^T \Omega \xi}, \quad \Omega = \bigoplus_{k=1}^N \begin{pmatrix} 0 & 1 \\ -1 & 0 \end{pmatrix}, \quad \xi \in \mathbb{R}^{2N}, \quad (15)$$

with $\mathbf{x} = (q_1, q_2, \dots, q_N, p_N)$ being the vector of quadrature operators. These N -mode displacement operators satisfy

$$\text{Tr}(D(\xi)D(\xi')) = \pi^N \delta(\xi + \xi'), \quad (16)$$

$$\frac{1}{\pi^N} \int d^{2N} \xi D(\xi) A D^{\dagger}(\xi) = \text{Tr}(A) \mathbf{I}. \quad (17)$$

The CV OTOC is defined to be

$$\mathcal{C}_2(\xi_1, \xi_2; t)_{\rho} = \text{Tr} [\rho D^{\dagger}(\xi_1; t) D^{\dagger}(\xi_2) D(\xi_1; t) D(\xi_2)] \quad (18)$$

where the so-called displacement operator takes the following form

$$D(\xi_2; t) = \frac{1}{\pi^N} \int d^{2N} \xi_2 \chi[\xi_2; D(\xi_1; t)] D(-\xi_2) \quad (19)$$

$$D(\xi_1; t) \equiv U(t)^{\dagger} D(\xi_1) U(t). \quad (20)$$

From the above decomposition, which is allowed by the completeness of displacement operators, one can infer that scrambling in the CV system is featured by the growth of the Wigner characteristic $\chi[\xi_2; D(\xi_1; t)]$ given by

$$\chi(\xi; A) \equiv \text{Tr}[AD(\xi)], \quad (21)$$

$$\chi[\xi_2; D(\xi_1; 0)] = \pi^N \delta(\xi_2 + \xi_1). \quad (22)$$

Now, given

$$\chi[\xi; D(\xi_1; t)] \sim e^{\frac{|\xi - \xi_1|^2}{2\mathcal{V}}} \quad (23)$$

and making use of the formulae presented above leads to (13). This proves that the decay of the OTOCs probes the increase in operator volume \mathcal{V} characteristic of scrambling. One should be able to directly relate the increase of the operator volume in the phase space with the size of the wormhole in the two entangled black holes model studied above rendering the connection between OTOC-LE and complexity more rigorous. This correspondence may be achieved by matching the norm of the displacement vector with the AdS radius, i.e., $|\xi| \sim 1/l_{AdS}$ (cf. eq.(8)).

It is worth emphasising that averaging the OTOCs over ensembles of displacement operators may enable us to measure a coarse-grained spread of a time-evolved operator in phase space. This may allow one to gain better understanding into the link between various diagnostics. For more about using the average OTOCs as probes for finer-grained aspects of operator distribution, we refer the reader to [36]. In section III we shall pursue a slightly different path to establish such a connection between the three diagnostics.

III. LOSCHMIDT ECHO AND COMPLEXITY

A. Introducing Complexity

Recently complexity has been demonstrated as an equally powerful and computationally simpler quantity in some cases than OTOC to diagnose the chaotic behaviour of a quantum system [11, 18]. Since all three of these quantities—LE, OTOC and Complexity—are providing similar information about the chaotic system, it is natural to anticipate that these three quantities are related to each other. In the previous sections we have established that the sub-system LE and averaged OTOC are the same. Therefore, to establish the relationship between the three quantities, we only need to explore the connection between LE and complexity.

To make progress in this direction, we will use the complexity for a particular quantum circuit from the inverted oscillator model as discussed in section II D. In [11], it was shown that the appropriate quantum circuit in this regard is the one where the target state $|\psi_2\rangle$ is obtained by evolving a reference state $|\psi_0\rangle$ forward in time by Hamiltonian H and then backward in time with slightly different Hamiltonian $H + \delta H$ as follows

$$|\psi_2\rangle = e^{i(H+\delta)t} e^{-iHt} |\psi_0\rangle. \quad (24)$$

For the inverted harmonic oscillator model the authors in [11] showed that the complexity evaluated by using the covariance matrix method [37, 38] for the above mentioned target state with respect to the reference state $|\psi_0\rangle$ is given by

$$C = \frac{1}{2} \left[\cosh^{-1} \left(\frac{\omega_r^2 + |\hat{\omega}(t)|^2}{2\omega_r \operatorname{Re}(\hat{\omega}(t))} \right) \right], \quad (25)$$

where $\hat{\omega}(t)$ is the frequency of the doubly evolved Gaussian target state which has the following form

$$\psi_2(x, t) = \hat{\mathcal{N}}(t) \exp \left[-\frac{1}{2} \hat{\omega}(t) x^2 \right], \quad (26)$$

and

$$\hat{\omega}(t) = \left[i \Omega' \cot(\Omega' t) + \frac{\Omega'^2}{\sin^2(\Omega' t)(\omega(t) + i \Omega' \cot(\Omega' t))} \right]. \quad (27)$$

In the last expression, $\Omega' = \sqrt{m^2 - \lambda'}$ is the frequency associated with the perturbed/slightly different Hamiltonian $H' = \frac{1}{2}p^2 + \frac{\Omega'^2}{2}x^2$ and $\lambda' = \lambda + \delta\lambda$ with $\delta\lambda$ very small. We make this perturbation by hand.

Note that the quantum circuit involving two time-evolutions with slightly different Hamiltonians is crucial for extracting the chaotic nature of the quantum system. Complexity for any target state will not capture similar information as OTOC. For example, the complexity of a target state which is forward evolved only once will not capture the scrambling time for the chaotic system as illustrated in Fig 9. However, there is an alternative

quantum circuit that will have the same complexity when evaluated by the covariance matrix method. In that circuit both the reference and target states are basically evolved states but with slightly different Hamiltonians from some other state. Once again this particular circuit also involves two evolutions.

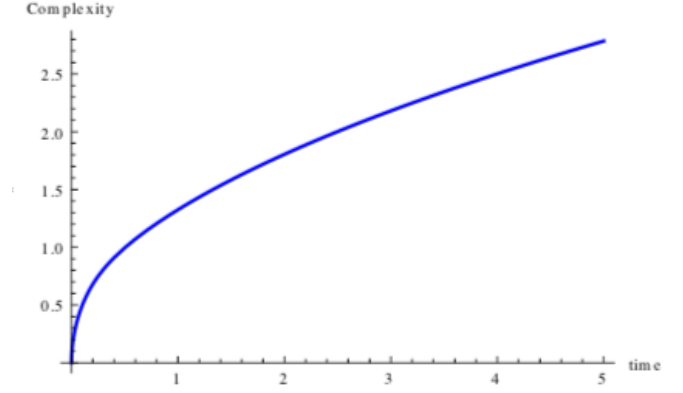


FIG. 9. Complexity of Single time evolved target state for Inverted Oscillator ($m = 1, \lambda = 20$).

B. LE-Complexity connection

It was shown in [11] that complexity of the above mentioned target state (24) can capture equivalent information such as scrambling time and Lyapunov exponent as the OTOC for an inverted oscillator. In this paper, we want to make this statement more precise by using the fact that averaged OTOC is the same as (very close to) the subsystem LE. In section II D of this paper, we have proved this for the Heisenberg group. In the current section, we will use an explicit example from the Heisenberg group, namely the inverted oscillator to demonstrate that LE for the full system and complexity are very close quantities.

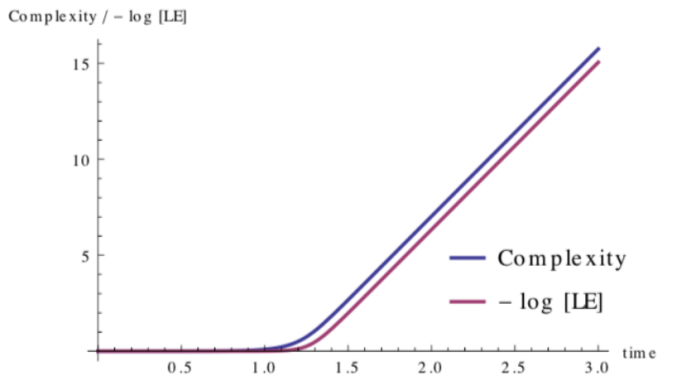


FIG. 10. Time evolution of negative logarithm of LE and Complexity for Inverted Oscillator ($m = 1, \lambda = 20, \delta\lambda = 0.001$)

It is noteworthy that the construction procedure of this quantum circuit is conceptually similar to the LE, where one basically computes the overlap between these above mentioned states. Complexity simply offers us a different measure for the distance which is a more powerful measure for understanding various properties of quantum systems [39–42].

As shown in Fig 3, the time evolution of LE has a flat portion for a while, which is followed by an exponential decay. On the other hand it takes a certain amount of time for complexity to pick up and then grow exponentially. These growth patterns are suggestive of the following relationship between LE and complexity for the above mentioned quantum circuit

$$\mathcal{C} = -\log [\text{LE}]. \quad (28)$$

To confirm our findings we plot the time evolution of Complexity and the $-\log [\text{LE}]$ as shown in Fig. 10. As predicted, these two quantities are remarkably close. They have exactly the same Lyapunov exponent (slope of the linear growth portion) and almost equal pick up time (scrambling time). This surprising equality is an indication of deeper physics surrounding these quantities and also provides a geometric meaning to the problem of quantum chaos.

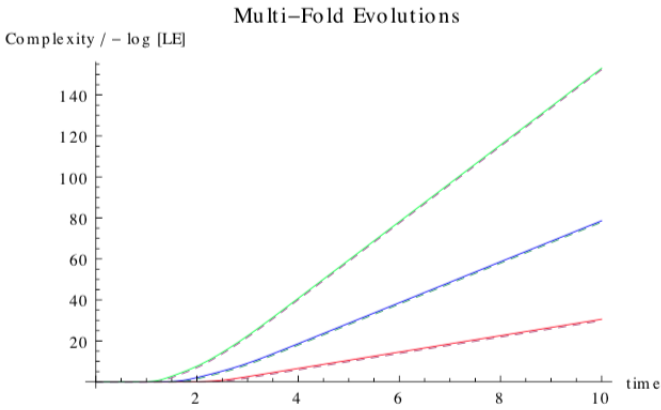


FIG. 11. Time evolution of negative of logarithm of Higher fold LE and Complexity for Inverted Oscillator ($m = 1, \lambda = 5$ (Green), 10 (Blue), 20 (Red), $\delta\lambda = 0.001$). The solid line is complexity and the dashed line is $-\log [\text{LE}]$.

We can easily generalize this particular construction of quantum circuit to relate it with $2(k-1)$ -fold LEs. The trick is to insert a pair of evolutions (forward and followed by a backward) for each fold of the echo. For example, for the 4-fold LE the quantum circuit we need to construct has the following form for the target state

$$|\psi_4\rangle = \underbrace{e^{i(H'+\delta)t} e^{-iH't}}_{\text{2nd pair of evolutions}} \underbrace{e^{i(H+\delta)t} e^{-iHt}}_{\text{1st pair of evolutions}} |\psi_0\rangle. \quad (29)$$

In figure 11 we show a few of the higher fold-LE ($-\log [\text{LE}]$, to be precise) and the corresponding generalization

of complexities. For each pair we see a clear match between complexity and the $-\log [\text{LE}]$. We do not have a concrete algebraic proof to establish the relationship at this point; we leave it for a future work.

Note that the sub-system LE that we have used in the previous sections can be quite close to full system LE, when the sub-system associated with the LE is much larger than the other one. We will conclude this section by making the assertion that these three diagnostics of chaos-averaged OTOC, LE and a particular type of complexity—are not only carrying similar information about the underlying quantum system, but also have some direct connection with each other.

IV. DISCUSSION

In this paper we have extended the proof that the averaged (Haar average over unitaries) OTOC is the same as the LE (for a sub-system) as in [14] to higher point averaged OTOC and LE for finite dimensional system. Moreover, we have also generalized the proof for Haar average to infinite dimensional case. We have shown that the OTOC-LE relation holds in other averaging scenarios as well, e.g., the Heisenberg group average, as long as the given group is a unitary 1-design. We argue that if the sub-system for this LE is much larger than the other sub-system, this LE would be essentially the same as the LE of the full system.

Furthermore, for an explicit example in the Heisenberg group we showed graphically that LE for the full system and Complexity for some special type of quantum circuit is the same. Finally, we have extended this result for multi-fold LE and corresponding extensions of the complexity. These different results suggest that these three diagnostics of a chaotic quantum system, namely averaged OTOC, LE and complexity are secretly the same. However, we do not have a concrete proof at this point. Tying complexity as an alternative probe to OTOC or LE also provides a geometric meaning to the chaotic behaviour of a quantum system.

To give a proof-of-principle argument for the similarity between complexity and LE, we have used the inverted oscillator as a toy model. This is, however, a rather special example and not a realistic chaotic system. Also, we used graphical techniques to establish our result. To claim that our particular complexity and LE (and hence averaged OTOC) are basically the same probe for understanding a quantum chaos will require a rigorous algebraic proof by using more realistic systems like the maximally chaotic SYK model and its many variants (see, for example, [43–45] and references therein).

Another possible extension of our work is to explore sub-system complexity in a system with N-inverted oscillators. This would help us make the connection between these quantities more rigorously.

ACKNOWLEDGMENTS

The authors would like to thank Aritra Banerjee, Jordan Colter, Jorge Kurchan and Dan Roberts for useful discussions and email exchanges. W.A.C would like to thank the Institute for Quantum Information and Matter (IQIM), Caltech, for the ongoing stimulating environment from which the author has been significantly benefited. W.A.C gratefully acknowledges the support of the Natural Sciences and Engineering Research Council of Canada (NSERC). B. Y. has been supported in part by the U.S. Department of Energy, Office of Science, Basic Energy Sciences, Materials Sciences and Engineering Division, Condensed Matter Theory Program. AB is supported by JSPS Grant-in-Aid for JSPS fellows 17F17023.

AUTHOR CONTRIBUTIONS

Please note that the authors' names are listed alphabetically. All authors contributed equally to this paper.

Appendix A: Mathematical Gear Oils

Here we define the mathematical tools that will be handy in the derivations to be performed. Those tools include

1. In Section II of the main text, a formula for the Haar average of a given trace-class operator O has been discussed. At finite dimension

$$\int_{\text{Haar}} dU(U^\dagger)OU = \frac{1}{d} \text{Tr}(O)I,$$

where I is the identity operator. The Hilbert space dimension d appears here because of the Haar measure is normalized by convention, $\int dU = 1$. At infinite dimension, a similar relation holds as well:

$$\int_{\text{Haar}} dU(U^\dagger)OU = \text{Tr}(O)I,$$

Here we present the formula for the Haar average of unitary operators restricted to a subsystem, which has been derived in Ref. ([14]). We only consider the finite dimensional case. For infinite dimensions

similar relations can be treated in the same manner.

$$\int_{\text{Haar}} dU_A(U_A^\dagger \otimes I_B O_{AB} U_A \otimes I_B)$$

we use $(A \otimes B)(C \otimes D) = (AC) \otimes (BD)$, to get

$$\begin{aligned} &= \int dU_A(U_A^\dagger \otimes I_B) \left(\sum_i O_i^A \otimes O_i^B \right) (U_A \otimes I_B) \\ &= \sum_i \int dU_A(U_A^\dagger O_i^A U_A \otimes O_i^B) \\ &= \frac{1}{d_A} \sum_i \text{Tr}(O_i^A) I_A \otimes O_i^B \end{aligned}$$

using $k(A \otimes B) = A \otimes (kB) = kA \otimes B$;

with k being scalar we obtain that

$$= \frac{1}{d_A} \sum_i I_A \otimes \text{Tr}(O_i^A) O_i^B$$

Finally, we reach the intended form which is

$$= \frac{1}{d_A} I_A \otimes \text{Tr}_A O_{AB}.$$

2. Reduced dynamics for local operators [14]:
Given a total system Hamiltonian

$$H = H_A \otimes I_B + I_A \otimes H_B + H_I,$$

where A denotes a small local subsystem S_A . B denotes the compliment of S_A to the total system, which is much larger compared to the local system S_A . We are interested in strongly coupled systems, where the energy scales admits a hierarchy $\bar{H}_A \ll \bar{H}_I \ll \bar{H}_B$. For instance, in a N -particle system with all-to-all two-body interactions, when the subsystem S_A refers to a single particle, the energy scales of S_A , S_B , and the coupling between them, are on the order of 1, N^2 and N , respectively. The interaction can be decomposed as

$$H_I = \lambda \sum_{i=1}^{d_A^2} V_A^i \otimes V_B^i.$$

Here we are free to chose the operators $\{V_A^i\}$ Hermitian and orthonormal, with respect to the Hilbert-Schmidt inner product, i.e.,

$$\text{Tr}(V_A^i V_A^j) = \delta_{i,j}.$$

The operators V_B^i on S_B are also Hermitian, but their (Hilbert-Schmidt) norms are fixed as equal to the norms of H_B . Thus, the parameter λ qualifies the relative strength of the coupling compared to H_B .

We are interested in the reduced dynamics of an operator B on the subsystem S_B , after the trace-out procedure, namely,

$$B(t) = \text{Tr}_A (e^{iHt} I_A \otimes B e^{-iHt}).$$

This can be thought of as a decoherence process, i.e., the total system is prepared in an initial product state $I_A \otimes B$, where the subsystem S_B has a “density matrix” B , and the subsystem S_A , up-to normalization, is in a thermal state with infinite temperature. The “quantum state” B will become “mixed” with time evolution due to the presence of the couplings to subsystem S_A . When $\lambda \ll 1$, the above evolution of $B(t)$ can be expanded to the second order of λ . This corresponds to the Born-Markov approximation, which leads the effective master equation for $B(t)$ to a Lindblad form. It is known that in this case the effective master equation can be simulated with the evolution of B under H_B without coupling to other systems, but subjects to a stochastic field

$$\lambda \mathcal{F}(t) = \lambda \sum_i l_i(t) V_B^i,$$

with the correlations given by

$$\begin{aligned} & \ll l_i(t) l_j(t - \tau) \gg \\ & = \text{Tr}(V_A^i e^{iH_A \tau} V_A^j e^{-iH_A \tau}) \\ & \approx \delta_{i,j}. \end{aligned}$$

[1] N. R. Hunter-Jones, Dissertation (Ph.D.), California Institute of Technology. doi:10.7907/BHZ5-HV76 (2018).

[2] V. Jahnke, *Adv. High Energy Phys.* **2019**, 9632708 (2019), arXiv:1811.06949 [hep-th].

[3] A. Larkin and Y. N. Ovchinnikov, *Sov Phys JETP* **28**, 1200 (1969).

[4] A. Kitaev, *Proceedings of the KITP Program: Entanglement in Strongly-Correlated Quantum Matter*, Kavli Institute for Theoretical Physics, Santa Barbara **7** (2015).

[5] A. Goussev, R. A. Jalabert, H. M. Pastawski, and D. Wisniacki, arXiv preprint arXiv:1206.6348 (2012).

[6] T. Gorin, T. Prosen, T. H. Seligman, and M. Žnidarič, *Physics Reports* **435**, 33 (2006).

[7] L. Susskind, (2018), arXiv:1802.01198 [hep-th].

[8] J. M. Magan, *JHEP* **09**, 043 (2018), arXiv:1805.05839 [hep-th].

[9] V. Balasubramanian, M. Decross, A. Kar, and O. Parrikar, (2019), arXiv:1905.05765 [hep-th].

[10] R.-Q. Yang and K.-Y. Kim, (2019), arXiv:1906.02052 [hep-th].

[11] T. Ali, A. Bhattacharyya, S. Shajidul Haque, E. H. Kim, N. Moynihan, and J. Murugan, (2019), arXiv:1905.13534 [hep-th].

[12] M. A. Nielsen, M. R. Dowling, M. Gu, and A. C. Doherty, *Science* **311**, 1133 (2006), arXiv:quant-ph/0603161 [quant-ph].

[13] R. Jefferson and R. C. Myers, *JHEP* **10**, 107 (2017), arXiv:1707.08570 [hep-th].

[14] B. Yan, L. Cincio, and W. H. Zurek, arXiv preprint arXiv:1903.02651 (2019).

[15] A. Romero-Bermúdez, K. Schalm, and V. Scopelliti, arXiv preprint arXiv:1903.09595 (2019).

[16] J. Kurchan, *Journal of Statistical Physics* **171**, 965 (2018).

[17] R. Fan, P. Zhang, H. Shen, and H. Zhai, arXiv e-prints , arXiv:1608.01914 (2016), arXiv:1608.01914 [cond-mat.quant-gas].

[18] J. Cotler, N. Hunter-Jones, J. Liu, and B. Yoshida, *JHEP* **11**, 048 (2017), arXiv:1706.05400 [hep-th].

[19] J. Maldacena, S. H. Shenker, and D. Stanford, *JHEP* **08**, 106 (2016), arXiv:1503.01409 [hep-th].

[20] D. A. Roberts and B. Yoshida, *J. High Energy Phys.* **2017**, 121 (2017).

[21] S. H. Shenker and D. Stanford, *J. High Energy Phys.* **2014**, 46 (2014).

[22] J. Cotler, N. Hunter-Jones, J. Liu, and B. Yoshida, *J. High Energy Phys.* **2017**, 48 (2017).

[23] R. de Mello Koch, J.-H. Huang, C.-T. Ma, and H. J. R. Van Zyl, *Phys. Lett.* **B795**, 183 (2019), arXiv:1905.10981 [hep-th].

[24] J. Li, R. Fan, H. Wang, B. Ye, B. Zeng, H. Zhai, X. Peng, and J. Du, *Phys. Rev.* **X7**, 031011 (2017), arXiv:1609.01246 [cond-mat.str-el].

[25] K. A. Landsman, C. Figgatt, T. Schuster, N. M. Linke, B. Yoshida, N. Y. Yao, and C. Monroe, *Nature* **567**, 61 (2019), arXiv:1806.02807 [quant-ph].

[26] M. Gärttner, J. G. Bohnet, A. Safavi-Naini, M. L. Wall, J. J. Bollinger, and A. M. Rey, *Nature Physics* **13**, 781 (2017).

[27] J. R. Gonzlez Alonso, N. Yunger Halpern, and J. Dressel, *Phys. Rev. Lett.* **122**, 040404 (2019), arXiv:1806.09637 [quant-ph].

[28] D. Stanford and L. Susskind, *Physical Review D* **90**, 126007 (2014).

[29] W. Chemissany and T. J. Osborne, *Journal of High Energy Physics* **2016**, 55 (2016).

[30] S. H. Shenker and D. Stanford, *Journal of High Energy Physics* **2014**, 46 (2014).

[31] D. A. Roberts, D. Stanford, and L. Susskind, *Journal of*

The approximation in the last step is due to the large energy hierarchy: the time scale of the dynamics of the subsystem S_A is much larger than that of $B(t)$ under consideration. Alternatively, this can be thought of as taking the zeroth order the H_A . As a consequence, the noise field $l_i(t)$ can be taken as random constant valued, ± 1 , at equal probability. The reduced dynamics of the B operator is then given by

$$B(t) = d_A \ll e^{-i(H_B + \lambda \mathcal{F})t} B e^{i(H_B + \lambda \mathcal{F})t} \gg,$$

averaged over the stochastic field. Note that the pre-factor d_A appears from the normalization of I_A . As the noise field are random ± 1 , each realization of the stochastic field \mathcal{F} in the above solution of $B(t)$ always appears as random combination of V_B^i ’s. Suppose that are totally N realizations, the noisy evolution of $B(t)$ is then

$$B(t) \approx d_A \times \frac{1}{N} \sum_{i,j=1}^N e^{-i(H_B + \lambda \mathcal{F}_k)t} B e^{i(H_B + \lambda \mathcal{F}_k)t}.$$

High Energy Physics **2015**, 51 (2015).

[32] L. Susskind, arXiv preprint arXiv:1810.11563 (2018).

[33] A. R. Brown, L. Susskind, and Y. Zhao, Physical Review D **95**, 045010 (2017).

[34] A. R. Brown and L. Susskind, Physical Review D **97**, 086015 (2018).

[35] B. Swingle, “Quantum information scrambling: Boulder lectures,” (2018).

[36] Q. Zhuang, T. Schuster, B. Yoshida, and N. Y. Yao, Physical Review A **99**, 062334 (2019).

[37] L. Hackl and R. C. Myers, JHEP **07**, 139 (2018), arXiv:1803.10638 [hep-th].

[38] H. A. Camargo, P. Caputa, D. Das, M. P. Heller, and R. Jefferson, Phys. Rev. Lett. **122**, 081601 (2019), arXiv:1807.07075 [hep-th].

[39] A. Bhattacharyya, A. Shekar, and A. Sinha, JHEP **10**, 140 (2018), arXiv:1808.03105 [hep-th].

[40] T. Ali, A. Bhattacharyya, S. S. Haque, E. H. Kim, and N. Moynihan, Journal of High Energy Physics **2019**, 87 (2019).

[41] T. Ali, A. Bhattacharyya, S. Shajidul Haque, E. H. Kim, and N. Moynihan, (2018), arXiv:1811.05985 [hep-th].

[42] A. Bhattacharyya, P. Nandy, and A. Sinha, (2019), arXiv:1907.08223 [hep-th].

[43] J. Maldacena and D. Stanford, Phys. Rev. **D94**, 106002 (2016), arXiv:1604.07818 [hep-th].

[44] W. Fu, D. Gaiotto, J. Maldacena, and S. Sachdev, Phys. Rev. **D95**, 026009 (2017), [Addendum: Phys. Rev.D95,no.6,069904(2017)], arXiv:1610.08917 [hep-th].

[45] A. Kitaev and S. J. Suh, JHEP **05**, 183 (2018), arXiv:1711.08467 [hep-th].